Synthesis and characterization of $n = 5$, 6 members of the $La_4Sr_{n-4}Ti_nO_{3n+2}$ series with layered structure based upon perovskite

Jesús Canales-Vázquez, John T.S. Irvine,* and Wuzong Zhou

School of Chemistry, University of St. Andrews, The Purdie Building, St. Andrews, Fife, Scotland KY16 9 ST, UK

Abstract

Layered compounds have been synthesized and structurally characterized for the $n = 5$ and 6 members of the perovskite-related family $La_4Sr_{n-4}Ti_nO_{3n+2}$ by combining X-ray diffraction and transmission electron microscopy. Their structure can be regarded as comprising $[(La,Sr)_5Ti_5O_{17}]$ and $[(La,Sr)_6Ti_6O_{20}]$ perovskite blocks joined by crystallographic shears along the a-axis, with consecutive blocks shifted by $1/2\,[100]_p$. The $n = 5$ member is similar to the previously reported $n = 5$ member of other $A_nB_nO_{3n+2}$-related series. The $n = 6$ member, which has only been briefly reported in other systems previously, is also a well-behaved member of this $A_nB_nO_{3n+2}$ series.
© 2004 Elsevier Inc. All rights reserved.

Keywords: $A_nB_nO_{3n+2}$ layered perovskites; HRTEM; XRD; Structural characterization

1. Introduction

Perovskite structures have been extensively investigated due to the important properties exhibited by many members of this series of materials. Layered perovskites are of great interest because extra oxygen beyond the ABO_3 stoichiometry is accommodated and their physico-chemical properties are therefore changed accordingly. There are several families of layered perovskites such as Ruddlesden–Popper [1], Aurivillius [2], Sillén [3] or Dion–Jacobson [4–5] phases which are based on the ability of perovskites to intergrow with rock salt layers, fluorite layers, e.g., $Bi[Bi_2O_2]^{2+}$, $[M_2O_2]X_2$ or AX halides (A: Cs^+, K^+, Rb^+), respectively. There is however a family of layered perovskites that is not based on intergrowths of different phases: the $A_nB_nO_{3n+2}$ series. The structures of these compounds can be described in terms of slabs containing n {110} perovskite layers joined by crystallographic shears along the $[100]_p$ direction. Consecutive blocks are shifted by $1/2[001]_p$ from each other (Fig. 1). The octahedra are tilted and strongly distorted as reported in the literature. The existence of such phases seems to be restricted to the lower n value members of titanates, niobates and tantalates (A: Nd, La, Ca, Sr, Ba, Na) as reported by Lichtenberg et al. [6] in a recent review. Most investigations have been focused on the $n = 4$ and 5 members of ternary systems such as $Nd_2Ti_2O_7$, $Ca_2Nb_2O_7$ or $La_5Ti_5O_{17}$. Examples of phases with $n>5$ are scarce and crystallographic studies based mainly on X-ray diffraction (XRD) are only known in the case of $Nd_4Ca_2Ti_6O_{20}$ and $La_4Ca_2Ti_6O_{20}$ investigated by Nanot et al. [7–8] two decades ago. Transmission electron microscopy (TEM) and XRD investigations were also performed by Levin et al. in $Sr_6Ti_2Nb_4O_{20}$ and $Sr_7Ti_3Nb_4O_{23}$, although the presence of well-ordered phases without stacking faults along the longest axis was not shown [9]. On the other hand, to the best of our knowledge, layered compounds in the $La_4Sr_{n-4}Ti_nO_{3n+2}$ system have not been reported as single or, at least, major phases.

In this communication, we report the synthesis and structural characterization of the $n = 5$ and 6 members of the $La_4Sr_{n-4}Ti_nO_{3n+2}$ series by means of XRD and high-resolution transmission electron microscopy (HRTEM). The system can be considered as being formed from intergrowths of the two end members, i.e., $La_2Ti_2O_7$ ($n = 4$) and $SrTiO_3$ ($n = \infty$), which would yield gradually larger perovskite slabs with increasing n. $SrTiO_3$ is a simple cubic perovskite with $a = 3.9059$ Å,

---

*Corresponding author. Fax: +44-1334-46-3808.

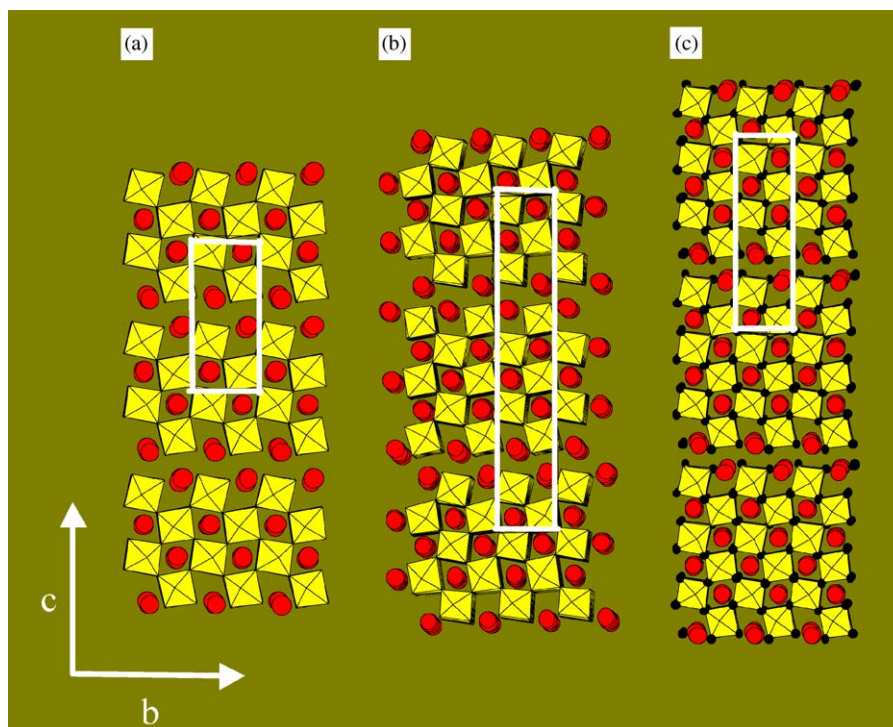*E-mail address:* jtsi@st-andrews.ac.uk, jtsi@st-and.ac.uk (J.T.S. Irvine).

Fig. 1. Schematic structural models for the $La_4Sr_{n-4}Ti_nO_{3n+2}$ series. (a) $La_2Ti_2O_7$ ($n = 4$), (b) $La_4SrTi_5O_{17}$ ($n = 5$), and (c) $La_4Sr_2Ti_6O_{20}$ ($n = 6$). The atomic positions for $La_2Ti_2O_7$ were taken from Ref. [10c], whereas for $n = 5$ and 6 were estimated by adding $\{110\}_p$ atomic layers using the same structural principle.

whilst $La_2Ti_2O_7$ has a monoclinic unit cell with parameters $a = 7.812(2)$ Å, $b = 5.544(1)$ Å, $c = 13.010(2)$ Å and $\beta = 98.66(1)$ [10] (Fig. 1a). Initial unit cell parameters were first estimated from selected area electron diffraction (SAED) and then more accurately using a least-squares method.

2. Experimental section

The samples were prepared by traditional solid-state reaction. Stoichiometric amounts of pre-dried high-purity La_2O_3, $SrCO_3$ and TiO_2 (Aldrich) were mixed and ground and then calcined at $1200°C$ for 6 h. The resulting powder was subsequently ground, mixed and uniaxially pressed into pellets, which were deposited on alumina crucibles containing sacrificial powder and then they were fired at $1400–1600°C$ for 3–9 days with intermediate processes of grinding, mixing and ''pelletizing''. XRD data were collected with a Stoe StadiP X-ray diffractometer, using $CuK\alpha_1$ radiation in the range $2\theta = 5-70°$ in steps of $0.1°$ at 300 s/step. HRTEM imaging and SAED were carried out using a JEOL-JEM 2011 electron microscope operating at 200 kV and equipped with a side entry $\pm 20°$ double tilt specimen holder. EDS microanalyses were performed using an Oxford Link ISIS system in at least 25 different crystals to confirm compositional homogeneity.

3. Results and discussion

Specimens of the $n = 5$ and 6 members were prepared under different conditions of reaction time and temperature as listed in Table 1 and thus the phase formation was monitored by means of both XRD and TEM. The $n = 5$ member could be produced using relatively short reaction times as happens for $La_2Ti_2O_7$, whilst the $n = 6$ member required extremely long annealing times to yield a major phase. That indicates the increased difficulty in achieving homogeneous samples when ordering in gradually larger perovskite blocks. The following discussion will only apply to samples a and d, which were essentially XRD single phase. EDS analyses confirmed for these specimens that the cation ratio corresponded to the expected stoichiometry with standard deviations of 10% or less, using high-purity $SrTiO_3$ and $La_2Ti_2O_7$ as standards.

SAED revealed that indeed most of the main zone axes of the $n = 5$ and 6 members resemble those of $La_2Ti_2O_7$ ($n = 4$). Dimensions of the c-axes of 31.3 (2×15.65 Å) and 18.5 Å were found, respectively, for the $n = 5$ and 6 members (Fig. 2), which corresponds to the addition of 1 and 2 $\{110\}_p$ layers per block, respectively. The doubling of the c-axis in $La_4SrTi_5O_{17}$ is probably explained by the very subtle modulation that exists between consecutive blocks when n is odd. This would be a consequence of the reverse tilting (canting)

Table 1
Reaction conditions and phase formation for the $n = 5$, 6 members of the $La_4Sr_{n-4}Ti_nO_{3n+2}$ series

Sample	Member	T (°C)	t (days)	$n = 4$	$n = 5$	$n = 6$	$n = \infty$	Other n
A	5	1500	3	—	D	—	T	—
B	6	1500	2	—	D	—	S	T
C		1500	2 + 2	—	S	T	S	T
D		1600	3 + 3 + 3	—	—	D	T	—

D: dominant; S: significant; T: traces. Significant means that they were observed by XRD, whereas traces indicate very small regions that could only be detected by HRTEM. $n = \infty$ indicates cubic perovskite. The reaction times are presented as the addition of consecutive steps separated by an intermediate process of grinding and mixing.
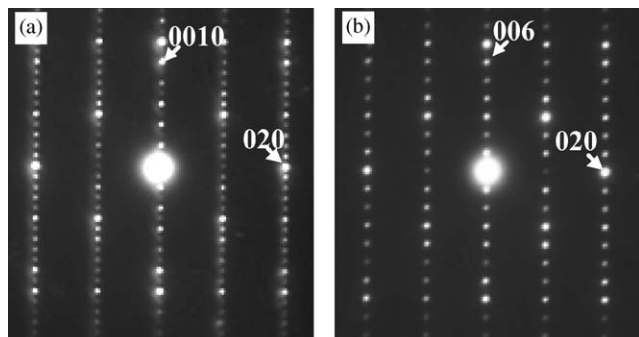

Fig. 2. SAED patterns corresponding to a view down the [100] projection for the $n = 5$ (a) and the $n = 6$ (b) members. There is no streaking along the c-axis, which is usually symptomatic of disorder.

between the layers of octahedra in two consecutive blocks as shown in Fig. 1b.

The HRTEM images taken down the $[120]_m$ projection reveal that the two compounds of interest are derived from regular perovskite blocks with 5 and 6 layers per block, respectively, joined by crystallographic shears along the c direction (Fig. 3). The bulk of the perovskite blocks present the hexagonal pattern (bright dots) that is characteristic of the $[111]_p$ projection of cubic structures. However, at the crystallographic shears the pattern is broken and two rows of atoms give a square pattern as marked with arrows, which is a consequence of the shift by $1/2 [001]_p$ between consecutive blocks. On those HRTEM images, it is also possible to distinguish the subtle modulation between consecutive blocks in the $n = 5$ member, which results in the doubling of the expected c parameter observed by SAED. In other words, the blocks are not crystallographically the same, but fall into two alternating types (X and Y) due to the different tilting orientations of octahedra (see Fig. 1) and have an arrangement of $XYXY$ along the c-axis. That doubling of blocks relieves the monoclinic distortion in the $n = 5$ member unit cell rendering it orthorhombic. The situation is somewhat different for the $n = 6$ member of the series ($La_4Sr_2Ti_6O_{20}$) because the number of layers per block is even. This case is analogous to the $n = 4$ member ($La_2Ti_2O_7$) because there is no reverse tilting of octahedra between consecutive blocks and hence the

c-axis is not doubled and the unit cell remains monoclinic. The perovskite blocks contain six layers each as shown by the HRTEM images. However, the monoclinic angle β is expected to change, becoming closer to 90° with increasing the number of layers per block. From simple geometric consideration of the additional layers per block in the repeat unit, one would estimate a β angle of 96.1 for the $n = 6$ member.

The XRD patterns from these two phases were indexed and the unit cell parameters estimated using a least-squares method taking the dimensions obtained from the TEM observations as initial parameters for the calculation as shown in Fig. 4, Tables 2 and 3. The patterns were indexed based upon the unit cell of $La_2Ti_2O_7$ ($n = 4$), having almost identical a- and b-axis and gradually larger c-axis, as a result of the already mentioned addition of one and two {110} perovskite layers per block, respectively. Both compounds seem to be single phase or at least very close to single phase since all peaks could be indexed on the unit cells proposed. A preliminary study of the systematic absences in both XRD and SAED suggested that the $n = 6$ member belongs to the same space group of $La_2Ti_2O_7$, i.e., $P2_1$ with the $(0k0)$ reflections not allowed when $k = 2n + 1$. This would agree with the model proposed by Nanot et al. [7] for $n = 6$ phases of the $Nd_2Ti_2O_7$–$CaTiO_3$ system. On the other hand, the $n = 5$ member seems to fit with the space group $P2_12_12_1$, with systematic absences $(h00)$, $(0k0)$ and $(00l)$ when h, k, and $l = 2n + 1$, respectively. This is also in agreement with Nanot's model. Previous studies for $n = 5$ phases of $Sr_5Nb_5O_{17}$ and $La_5Ti_5O_{17}$ have reported space groups of $Pnnm$ and Pc, respectively [11–14]; however, these are based upon a unit cell with $a = 3.95$ Å rather than $a = 7.8$ Å and are clearly inconsistent with the observed diffraction data for $La_4SrTi_5O_{17}$.

In conclusion, new layered perovskites belonging to the $La_4Sr_{n-4}Ti_nO_{3n+2}$ series have been synthesized and structurally characterized, showing the possibility of modulating the size of the perovskite blocks. It should be noted however that an increased difficulty in obtaining homogeneous samples must be expected for larger slabs. Indeed, our efforts in the synthesis and characterization of the $n = 8$ and 10 members resulted in a mixture of diverse-sized perovskite blocks irregularly
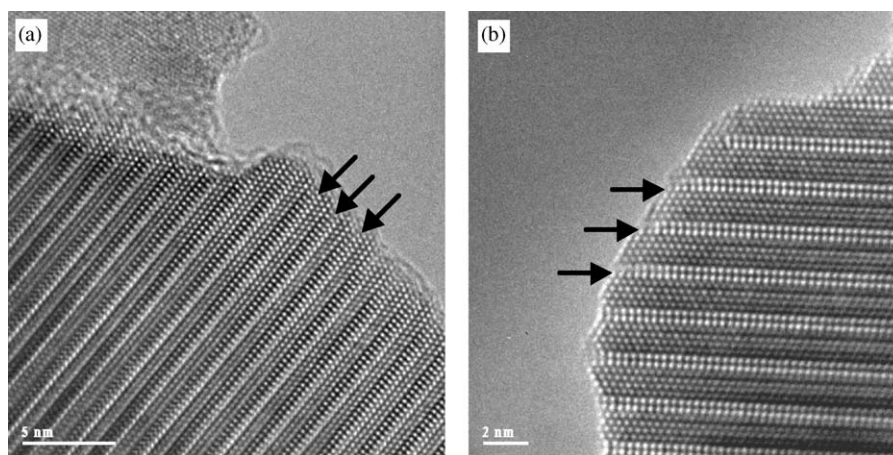
Fig. 3. HRTEM images viewing down the [120] zone axis for the $n = 5$ (a), and the $n = 6$ (b) members. In the case of the $n = 5$ member there are five layers per block, whilst there are six layers in the case of the $n = 6$ member. The arrows indicate the crystallographic shears.
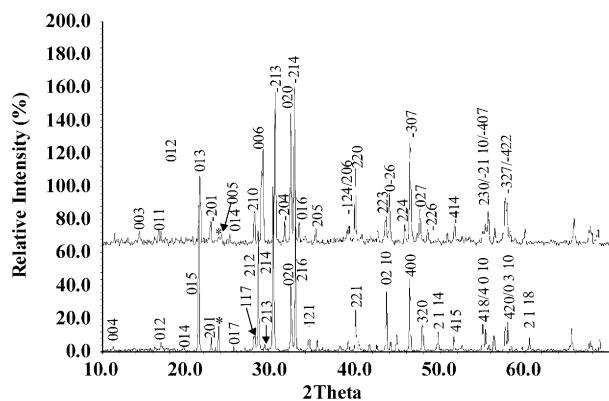

Fig. 4. XRD patterns for (a) $La_4SrTi_5O_{17}$, and (b) $La_4Sr_2Ti_6O_{20}$. * Indicates vaseline peaks. Not all the peaks appear in this figure due to the large number of peaks at very close 2θ values.

Table 2
Unit cell parameters for the $La_4Sr_{n-4}Ti_nO_{3n+2}$ series

n	Formula	a (Å)	b (Å)	c (Å)	β
4	$La_2Ti_2O_7$	7.812(2)	5.544(1)	13.01(1)	98.66(1)
5	$La_4SrTi_5O_{17}$	7.824(1)	5.536(1)	31.337(4)2)	90
6	$La_4Sr_2Ti_6O_{20}$	7.821(1)	5.541(1)	18.549(3)	96.1(1)

distributed within the crystals when reacted for insufficient periods of time, typically 72 h at 1500°C. Therefore, very long annealing periods of time at high temperature (1500–1600°C) are required to synthesize fairly pure higher members of this series of layered perovskites. Interesting properties such as ferroelectricity with very high T_c can be expected from this series, considering that the $n = 4$ member, $La_2Ti_2O_7$, is the ferroelectric material with the highest T_c (1770 K) reported [15]. Preliminary measurements do indicate that the $n = 6$ member is ferroelectric, but not the $n = 5$

Table 3
XRD powder data for the $n = 5$ (a) and $n = 6$ (b) members using a least-squares calculation

2θ (obs)	$h\,k\,l$	2θ (calc)	Int	d (obs)	d (calc)
(a)					
5.639	0 0 2	5.636	36	15.66	15.67
11.276	0 0 4	11.285	27	7.841	7.834
16.967	0 1 2	16.971	28	5.222	5.220
19.610	0 1 4	19.619	27	4.523	4.521
21.412	0 1 5	21.397	99	4.147	4.149
22.884	2 0 1	22.890	30	3.883	3.882
25.554	0 1 7	25.568	19	3.483	3.481
27.917	2 1 0	27.903	23	3.193	3.195
28.040	1 1 7	28.032	11	3.180	3.181
28.477	2 1 2	28.489	78	3.132	3.131
29.205	2 1 3	29.206	17	3.055	3.055
30.188	2 1 4	30.185	100	2.958	2.958
32.311	0 2 0	32.314	40	2.768	2.768
32.834	2 1 6	32.835	77	2.726	2.726
34.461	1 2 1	34.458	15	2.601	2.601
35.418	0 2 5	35.420	8	2.532	2.532
38.130	3 1 0	38.111	4	2.358	2.359
39.086	2 0 11	39.083	7	2.303	2.303
39.963	2 2 1	39.970	26	2.254	2.254
40.277	2 1 10	40.280	6	2.237	2.237
41.579	3 0 8	41.566	5	2.170	2.171
42.479	2 1 11	42.479	4	2.126	2.126
43.596	0 2 10	43.590	37	2.074	2.075
44.085	2 0 13	44.091	6	2.053	2.052
44.812	3 1 8	44.808	10	2.021	2.021
46.375	4 0 0	46.383	44	1.956	1.956
47.871	3 2 0	47.881	17	1.899	1.898
49.697	2 1 14	49.693	12	1.833	1.833
51.607	4 1 5	51.617	9	1.770	1.769
54.995	4 1 8	54.986	17	1.668	1.669
55.320	4 0 10	55.320	14	1.659	1.659
56.325	2 3 4	56.311	10	1.632	1.632
57.654	4 2 0	57.658	15	1.598	1.598
57.951	0 3 10	57.947	18	1.590	1.590
60.520	2 1 18	60.514	8	1.529	1.529
65.523	4 1 14	65.527	14	1.424	1.423
67.676	0 3 15	67.688	7	1.383	1.383
68.837	4 2 12	68.841	8	1.363	1.363

Table 3 (*continued*)

2θ (obs)	h k l	2θ (calc)	Int	d (obs)	d (calc)
(b)					
14.401	0 0 3	14.395	8	6.146	6.148
16.676	0 1 1	16.692	9	5.312	5.307
21.575	0 1 3	21.573	43	4.116	4.116
22.841	−2 0 1	22.849	15	3.890	3.889
24.110	0 0 5	24.107	6	3.688	3.689
25.116	0 1 4	25.105	7	3.543	3.544
28.012	2 1 0	28.011	21	3.183	3.183
28.419	2 0 3	28.408	8	3.138	3.139
29.020	0 0 6	29.025	60	3.075	3.074
30.468	−2 1 3	30.459	98	2.932	2.932
31.588	−2 0 5	31.586	15	2.830	2.830
32.308	0 2 0	32.285	78	2.769	2.771
32.755	−2 1 4	32.745	100	2.732	2.733
33.298	0 1 6	33.305	14	2.689	2.688
34.017	0 0 7	33.998	5	2.633	2.635
35.237	2 0 5	35.240	9	2.545	2.545
38.981	−1 2 4	39.015	11	2.308	2.307
39.198	2 0 6	39.208	12	2.296	2.296
39.930	2 2 0	39.923	48	2.256	2.256
40.692	0 2 5	40.696	6	2.216	2.215
41.756	2 2 2	41.761	5	2.162	2.161
42.583	2 1 6	42.591	8	2.121	2.121
43.527	2 2 3	43.533	18	2.078	2.077
43.958	0 2 6	43.961	32	2.058	2.058
45.801	2 2 4	45.809	13	1.980	1.979
46.420	−3 0 7	46.423	64	1.955	1.954
47.260	0 1 9	47.252	7	1.922	1.922
47.584	0 2 7	47.588	22	1.909	1.909
48.515	−2 2 6	48.518	10	1.875	1.875
50.809	−2 1 9	50.811	8	1.796	1.796
51.704	−4 1 4	51.709	13	1.767	1.766
55.006	2 3 0	54.994	8	1.668	1.668
55.316	−2 1 10	55.312	13	1.659	1.660
55.652	−4 0 7	55.649	21	1.650	1.650
56.438	−2 3 3	56.441	10	1.629	1.629
57.391	1 0 11	57.388	7	1.604	1.604
57.667	−3 2 7	57.675	30	1.597	1.597
57.887	−4 2 2	57.891	27	1.592	1.592
58.273	−4 1 7	58.291	8	1.582	1.582
60.032	−2 1 11	60.042	9	1.540	1.540
65.827	−4 2 7	65.817	17	1.418	1.418
67.682	5 1 4	67.675	11	1.383	1.383
68.647	−4 2 8	68.633	10	1.366	1.366

member, consistent with the proposed reverse tilting of the octahedral blocks in this phase.

Acknowledgments

References

[1] S.N. Ruddlesden, P. Popper, Acta Crystallogr. 10 (1957) 538.

[2] B. Aurivillius, Ark. Kemi. 1 (1949) 499.

[3] L.G. Sillén, Z. Anorg. Allg. Chem. 246 (1941) 331.

[4] M. Dion, M. Ganne, M. Tournoux, Mater. Res. Bull. 16 (1981) 1429.

[5] A.J. Jacobson, J.W. Johnson, J.T. Lewandowski, Inorg. Chem. 24 (1985) 3727.

[6] F. Lichtenberg, A. Herrnberger, K. Wiedenmann, J. Mannhart, Progr. Solid State Chem. 29 (2001) 1–70.

[7] M. Nanot, F. Queyroux, J.C. Gilles, R. Portier, J. Solid State Chem. 38 (1981) 74.

[8] M. Nanot, F. Queyroux, J.C. Gilles, J.J. Capponi, J. Solid State Chem. 61 (1986) 315.

[9] I. Levin, L.A. Bandersky, T.A. Vanderah, R.S. Roth, O.M. Stafsudd, Mater. Res. Bull. 33 (3) (1998) 501.

[10] (a) M. Gasperin, Acta Crystallogr. B 31 (1975) 2129.
    (b) N. Ishizawa, F. Narumo, T. Kawamura, M. Kimura, Acta Crystallogr. B 31 (1975) 1912.
    (c) H.W. Schmalle, T. Williams, A. Reller, A. Linden, J.G. Bednorz, Acta Crystallogr. B 49 (1993) 235.

[11] S.C. Abrahams, H.W. Schmalle, T. Williams, A. Reller, D. Widmer, J.G. Bednorz, R. Spreiter, Acta Crystallogr. B 54 (1998) 399.

[12] A.R. Drews, W. Wong-Ng, R.S. Roth, T.A. Vanderah, Mater. Res. Bull. 31 (1996) 153.

[13] T. Williams, H.W. Schmalle, A. Reller, F. Lichtenberg, D. Widmer, J.G. Bednorz, J. Solid State Chem. 93 (1991) 534.

[14] H.W. Schmalle, T. Williams, A. Reller, Acta Crystallogr. C 51 (1995) 1243.

[15] S. Nanamatsu, M. Kimura, K. Doi, S. Matsushita, N. Yamada, Ferroelectrics 8 (1974) 511.